



The role of tungsten oxide in the selective hydrogenolysis of glycerol to 1,3-propanediol over Pt/WO_x/Al₂O₃

Sara García-Fernández^{a,*}, Inaki Gandarias^a, Jesús Requies^a, Fouad Soulimani^b, Pedro L. Arias^a, Bert M. Weckhuysen^b

^a Department of Chemical and Environmental Engineering, Faculty of Engineering, University of the Basque Country (UPV/EHU), Alameda Urquijo Street s/n, 48013 Bilbao, Spain

^b Inorganic Chemistry and Catalysis, Debye Institute for Nanomaterials Science, Utrecht University, Universiteitsweg 99, 3584 CG Utrecht, The Netherlands

ARTICLE INFO

Article history:

Received 16 September 2016

Received in revised form 8 November 2016

Accepted 10 November 2016

Available online 11 November 2016

Keywords:

Tungsten oxide

Hydrogenolysis

Glycerol

1,3-Propanediol

ATR-IR spectroscopy

ABSTRACT

Bi-functional heterogeneous catalysts combining a noble metal with an oxophilic metal (mainly W or Re) were reported to be selective for the C–O hydrogenolysis of glycerol to the high added-value 1,3-propanediol. Despite intensive research work carried out, there is a great deal of controversy about the role of the oxophilic metal. In this work, the hydrogenolysis of glycerol over Pt/WO_x/Al₂O₃ catalysts was studied in real time by *in-situ* attenuated total reflection infrared (ATR-IR) spectroscopy. Moreover, *ex-situ* ATR-IR spectroscopic studies were also used to study the interactions between glycerol and the different catalytic surfaces. The results obtained indicate a stronger adsorption of glycerol through the primary hydroxy group/s when tungsten oxides are grafted onto the γ -Al₂O₃ support. The competitive adsorption between the reactant and the main reaction products for the same active sites, and the effect of the hydrogen availability were also studied. The evidences found in this work point out a triple role of tungsten oxide in the reaction, acting as: (i) a strong anchoring site for the primary hydroxy group/s of glycerol, (ii) a supplier of protons, and (iii) a stabilizer of the secondary carbocation. Under the best conditions, a remarkable high yield of 1,3-propanediol of 38.5% was obtained after only 4 h of reaction time.

© 2016 Elsevier B.V. All rights reserved.

1. Introduction

In a future sustainable scenario most of the useful chemicals will be produced from biomass-based platform molecules. A common characteristic of these compounds is that they have higher O/C ratio than most commodity chemicals, and hence they should be deoxygenated in order to yield high added-value products [1]. The C–O bond hydrogenolysis is one of the best approaches in the deoxygenation of these compounds. In this sense, the C–O hydrogenolysis of glycerol has attracted a great deal of attention in recent years, since glycerol is abundantly obtained as a by-product in the biodiesel manufacture through the transesterification of vegetable oils [2,3]. The interest in this reaction does not only come from the high industrial value of the chemical products obtained, but it is also considered as a model reaction of the reduction of more complicated biomass-related molecules. Among the two propane-diols (PDO) that can be obtained from glycerol hydrogenolysis,

1,3-PDO is commercially the most valuable. It is used as conventional functional fluid in cosmetics, personal care and cleaning products, but most of the 1,3-PDO is used as a monomer together with terephthalic acid to produce poly-trimethylene terephthalate (PTT) polymers [3,4]. The targeted market of 1,3-PDO is currently over 2.7 billion per year [5], and has traditionally been synthesized from fossil feedstock through two main routes: hydrolysis of acrolein and hydroformylation of ethylene oxide. The catalytic hydrogenolysis of glycerol appears to be an attractive and greener alternative to the current petroleum-based manufacturing methods.

Nevertheless, the selective formation of 1,3-PDO is very challenging and 1,2-PDO is commonly the main product obtained from the hydrogenolysis of glycerol. Although 1,2-PDO is also a valuable compound, widely used as functional fluid and especially as intermediate for the manufacture of unsaturated polyester resins and plastics, the difference of market price between glycerol and 1,2-PDO is relatively small [6].

Tuning of the 1,3-PDO/1,2-PDO ratio requires the use of catalytic systems highly selective for the C–O cleavage of the secondary (2°) or primary (1°) hydroxy (OH) groups of glycerol. High yields

* Corresponding author.

E-mail address: sara.garciaf@ehu.eus (S. García-Fernández).

of 1,2-PDO ($\geq 90\%$) have been reported [7–11] using typically bi-functional systems, formed by a hydrogenation metal and an acid or base additive, but the selective formation of 1,3-PDO requires the design of novel catalyst formulations. In the last years, the combination of a highly reducible noble metal with an oxophilic metal (mainly Re or W) [12–14] has opened the window to a new class of bi-functional heterogeneous catalysts for the selective C–O hydrogenolysis of glycerol.

The Tomishige's group proved the positive effect that the addition of ReO_x to different supported noble metals (*i.e.*, Rh, Ir, Pt, Pd and Ru on SiO_2) had on the selectivity towards 1,3-PDO [15–18]. The highest yield of 1,3-PDO was obtained over an Ir– ReO_x / SiO_2 catalyst (38%) at 120°C , 80 bar of H_2 and 36 h [15]. They propose the formation of two different kinds of glycerol alkoxides during the adsorption step, regarding the position of the OH group through which it is attached to the catalyst surface: *i.e.* a 1° alkoxide that would lead to 1,3-PDO formation and a 2° alkoxide that would lead to 1,2-PDO formation. According to the authors, the preferential terminal alkoxide formation on the ReO_x , due to a steric effect induced by the large Re clusters, could explain the high selectivities towards 1,3-PDO found [12,15,19].

Daniel et al. combined Pt and ReO_x supported on C (Pt– ReO_x /C) and also found a promoting effect of Re in the selective production of 1,3-PDO from glycerol [13]. The best result (*i.e.*, a 13% yield of 1,3-PDO) was obtained with a catalyst synthetized at elevated temperatures (700°C), which resulted in a better atomic mixing of the Pt and Re components without severely decreasing the metals dispersion. Regarding the role of the oxophilic ReO_x clusters, Daniel et al. proposed, without going into much detail, that they might facilitate the glycerol hydrogenolysis by the direct activation of a C–OH bond.

Chia et al. studied the C–O hydrogenolysis of polyols (glycerol among others) and cyclic-ethers derived from biomass over Rh– ReO_x /C [14]. The catalyst materials proved to be selective in the hydrogenolysis of the 2° C–O bonds. In view of the results obtained from density functional theory (DFT) calculations, the authors suggested that the OH groups on Re atoms associated with Rh are acidic, due to the strong Re–O bond formation, resulting in a weak O–H bond as well as high electron affinity for the conjugate base. These groups would be responsible for proton donation leading to the formation of carbenium ion transition states. These three disparate hypotheses described above reveal that there is still uncertainty about the role of the oxophilic metal in the selective production of 1,3-PDO.

In spite of the quite high yields of 1,3-PDO reported with ReO_x the use of WO_x is preferred, because it avoids most of the main problems of stability associated to the use of ReO_x [20]. Unlike ReO_x , they are almost insoluble in water and significantly higher temperatures are required to completely reduce the WO_x species. Thus, more robust and stable W-based catalytic systems appear as a better option for the aqueous phase valorization of glycerol. Kaneda et al. reported by far the highest yield of 1,3-PDO to date using Pt and WO_3 supported on "boehmite" catalyst (denoted as Pt/ WO_3 /Al(OH)) [21]. This value was 66% at complete glycerol conversion, at 180°C , 50 bar of H_2 and after 12 h reaction time. In spite of the extraordinary results obtained, the hypothesis postulated by the authors remains controversial. They attributed the high yield to the plentiful Al–OH groups in the boehmite support, which would promote the formation of Al-alkoxide species. However, the high reaction temperatures used in the catalyst pre-treatment (800°C) and the X-ray diffraction (XRD) patterns indicate a different alumina structure than boehmite (possibly γ - Al_2O_3) and, therefore, the presence of a limited number of OH groups.

In our work, the glycerol hydrogenolysis was studied using Pt/ WO_x /Al₂O₃ catalytic systems, which proved to be very effective in the reaction under study [22], in order to shed light into the role

of the oxophilic metal. For this purpose, the *in-situ* attenuated total reflection infrared (ATR-IR) spectroscopy was applied to the C–O hydrogenolysis of glycerol into PDO in the aqueous phase aiming to study the nature of the adsorbed species on the catalyst surface. The use of this technique avoids the direct transmission of the beam through the sample since the evanescent wave, generated after the total reflection of the infrared (IR) beam onto an internal reflection element (IRE), is restricted to a region near the solid-liquid interface (of only few microns). In this way, it allows studying the reaction on the catalyst surface and the liquid interference is minimized while maximizing the signals of the surface species [23,24].

Nevertheless, only a limited number of studies of the application of *in-situ* ATR-IR spectroscopy to aqueous phase chemical reactions have been reported to date. An illustrative example of the potential of this technique is the work of Dumesic et al. [25]. They combined the ATR-IR technique with a kinetic study in order to understand the differences between the reforming of methanol over a Pt/Al₂O₃ catalyst in vapor or aqueous-phase reaction conditions. More recently, Lefferts and co-workers applied this technique in the CO adsorption and aqueous phase oxidation, as well as in the nitrite hydrogenation, over noble metal supported catalysts, to determine the type of adsorbates and the possible reaction intermediates [26,27]. Moreover, *ex-situ* ATR-IR spectroscopy was also applied in our work to study the adsorption modes of glycerol on different catalyst surfaces. In addition, the combination of these spectroscopic techniques with a kinetic study and the use of different reacting atmospheres lead to the better understanding of the key role of the oxophilic metal in the reaction.

2. Experimental

2.1. Catalyst synthesis

The Pt/ WO_x /Al₂O₃ catalysts were prepared by sequential wetness impregnation (WI) method. The typical procedure followed for catalysts preparation is detailed below. The commercially available γ -Al₂O₃ (Merck, $\geq 99.9\%$) was used as support, and it was impregnated using the appropriate amounts of ammonium metatungstate ((NH_4)₆(H₂W₁₂O₄₀)-nH₂O, Sigma-Aldrich, $\geq 99.99\%$) dissolved in deionized water. Impregnated samples were dried at 110°C overnight and subsequently calcined in air from room temperature (RT) up to 450°C at a heating rate of 2°C min^{-1} . This temperature was hold for 4 h. Pt was then loaded on supported tungsten oxide catalysts by WI method using tetraammineplatinum (II) nitrate ($\text{Pt}(\text{NH}_3)_4(\text{NO}_3)_2$, Sigma-Aldrich, $\geq 99.995\%$) as precursor. The resulting catalysts were dried and calcined following the same procedure as above at 300°C . Henceforth, the prepared Pt/ WO_x /Al₂O₃ samples by WI are denoted as xPt_yWAl, where x refers to the real Pt content in weight percent (wt%) in the final catalyst and y to the W content related to the γ -Al₂O₃ support (in terms of wt% of W/ γ -Al₂O₃), both measured by inductively coupled plasma optical emission spectrometry (ICP-OES). The textural properties of the prepared samples obtained by N₂ physisorption are given in Table 1.

2.2. Catalyst layer deposition on the IRE

In a first step, aqueous solutions of the catalyst materials were prepared. For this purpose, Milli-Q water was first degassed for 2 h in order to remove the dissolved O₂, using a glass bubbler and a flow of pure Ar at RT. Typically, 50 mg of reduced catalyst (reduction conditions: 5°C min^{-1} up to 300°C with a flow of 100 mL min^{-1} of pure H₂ for 1 h) were finely crushed and added to 10 mL of degassed-water. To prepare a homogeneous aqueous suspension of the catalyst, the mixture was stirred in a sonicator for 24 h at RT. For

Table 1Overview of the nomenclature and the textural properties of the prepared Pt/WO_x/Al₂O₃ catalysts.

Sample code	Pt loading (wt%)	W loading (wt%) ^a	Surface area (m ² g ⁻¹)	Pore volume (cm ³ g ⁻¹)
Al	0	0	140	0.26
8WAl	0	8.5	110	0.20
9Pt8WAl	8.9	8.0	95	0.15

^a W loading related to the Al support.

the catalyst immobilization, two drops of the catalyst suspension were deposited on the internal reflection element (IRE). The water was then evaporated in a vacuum desiccator for 1 h. The process was repeated until a homogeneous layer was obtained and the IRE was completely covered. This method conducts to the preparation of steady layers as it was reported in previous works [25,28].

2.3. In-situ ATR-IR spectroscopic measurements

The *in-situ* ATR-IR spectroscopic measurements were conducted in a ReactIR 45 m FT-IR spectrometer (Mettler Toledo) equipped with a liquid N₂-cooled mercury cadmium telluride (MCT) detector. This equipment is an *in-situ* mid-infrared based system that allows monitoring the reaction in real time and, thus, obtaining a deeper and real reaction information. It is connected to an autoclave, in which the reaction is performed, through a K4 conduit to sentinel. The silicon (Si) crystal used as IRE, placed at the bottom of the autoclave, was coated with the catalyst layer prepared as explained above (Section 2.2).

The reactant solution, typically 20 mL of glycerol (Sigma-Aldrich, 99.0%) in Milli-Q water was placed in the autoclave. The glycerol concentration varied from 5 to 30 wt%, but the catalyst to glycerol ratio was kept constant (0.166 g_{catalyst} g⁻¹ reactant). Prior to the activity test, the catalyst was *ex-situ* reduced (see conditions in Section 2.2) and introduced into the autoclave in powder form (420–500 µm). The reactor was then purged 5 times with H₂. Afterwards, the pressure was increased up to the 35 bar and heating and stirring (550 rpm) started. The reaction began when the temperature and pressure reached the operation values of 200 °C and 45 bar.

The liquid and gaseous samples were taken when reaction finished, at 16 h reaction time, and after the system was cooled down (T < 40 °C). The composition of the gas phase was analyzed in a micro GC (Varian, 490 GC) equipped with a COX 1 m and a CP-Sil-5CB 6 m columns (Agilent Technologies). The liquid sample was analyzed using 1,4-butanediol (Sigma-Aldrich, 99.9%) as standard with a GC-TCD-FID (Agilent Technologies, 7890 A) equipped with a Meta-Wax capillary column (diameter 0.53 mm, length 30 m).

During the experiments, ATR-IR spectra were collected every 2 min for 6 h, at 15 min for the next 2 h and every 30 min for the other 8 h. The measurements were also performed during the heating. Each spectrum was collected using a resolution of 4 cm⁻¹ and 64 scans in the 4000–650 cm⁻¹ scan region. Blank-experiments were carried out following the same procedure but using the pure solvent as reactant (Milli-Q water).

2.4. Ex-situ ATR-IR spectroscopic measurements

The surface chemistry of a selection of catalysts (*i.e.*, Al and 8WAl) was also studied with *ex-situ* ATR-IR spectroscopy. The measurements were carried out in a TENSOR 37 instrument (from Bruker) equipped with a horizontal ATR accessory (FastIR from Harrick), a MCT detector and a zinc selenide (ZnSe) crystal as IRE. Typically, the catalyst was immobilized on the IRE surface as explained in Section 2.2. Its spectrum was recorded and used as background. Then, a drop of a glycerol aqueous solution (0.5–5.0 wt%), or water, was deposited over the catalyst layer and

the spectrum was collected. In some specific cases, the water spectrum was subtracted from the spectrum of the glycerol solution, both loaded over the same catalyst. In other measurements, after glycerol loading, the moisture of the layer was removed under high vacuum (HV) for 1 h. Then, the spectra were measured at room temperature and ambient pressure.

All ATR-IR spectra were recorded at 4 cm⁻¹ of resolution and 64 scans per spectrum in the 4000–650 cm⁻¹ region. In order to note vibrational shifts, the IRE was also fully covered by pure glycerol (Sigma-Aldrich, 99.0%).

2.5. Kinetic measurements and pressure effect

Kinetic studies were carried out in 4 similar stainless steel autoclaves of 50 mL capacity (RWTH Aachen University, Germany). Typically, 0.08 g (0.166 g_{catalyst} g⁻¹ glycerol) of *ex-situ* reduced 9Pt8WAl catalyst (reduction conditions in Section 2.2) and 10 mL of reactant solution were placed in each autoclave. The feed was modified in each experiment and its composition is specified during the discussion of results. The systems were then purged and pressurized up to 25 bar of H₂. Afterwards, they were placed in preheating heater plates with magnetic stirring of 550 rpm and heated up to 200 °C reaching a final pressure of 45 bar. After 2 h of reaction time the autoclaves were immediately cooled down in an ice-bath. A known amount of 1,4-butanediol (Sigma-Aldrich, 99.99%) aqueous solution was added to the reaction mixture as external standard, and a sample was then taken and analyzed in a GC-TCD-FID (6890 N, Agilent Technologies) equipped with a Supra-Wax capillary column (diameter 0.53 mm, length 30 m).

The same setup and a similar experimental process to the previously described were employed for the study of the H₂ pressure effect on the glycerol conversion and product distribution. For this purpose, 10 mL of 20 wt% glycerol in water and 0.2 g of the 9Pt8WAl catalyst (0.100 g_{catalyst} g⁻¹ reactant ratio) were employed. After the feed was placed into the autoclaves, they were pressurized at different initial H₂ pressures of 30, 45 and 55 bar, and then heated until 200 °C, reaching the final H₂ pressures of 50, 80 and 90 bar, respectively. The reaction took place for 4 h, after which the liquid samples were analyzed according to the procedure explained above.

2.6. Hydrogenolysis of glycerol and propanediols under different reacting atmospheres

These activity tests were carried out in a 50-mL stainless steel autoclave (PID Eng&Tech, Spain) with a stirring rate of 550 rpm. Typically, 0.35 g of catalyst powder (300–500 µm) was introduced into a catalytic basket inside the autoclave (0.166 g_{catalyst} g⁻¹ reactant ratio).

Prior to the activity test, the catalyst was *in-situ* reduced (conditions in Section 2.2). After reduction, the reactor was cooled down to the reaction temperature (220 °C) and the H₂ or N₂ pressure was increased up to 20 bar. Usually, 42 mL of 5 wt% aqueous reactant solution, glycerol (Sigma-Aldrich, 99.9%), 1,2-propanediol (Sigma-Aldrich, 99.9%) or 1,3-propanediol (Sigma-Aldrich, 98.0%), were placed into a feed cylinder under 50 bar of H₂ (or N₂) pressure. The feed was introduced into the reactor taking advantage of the pres-

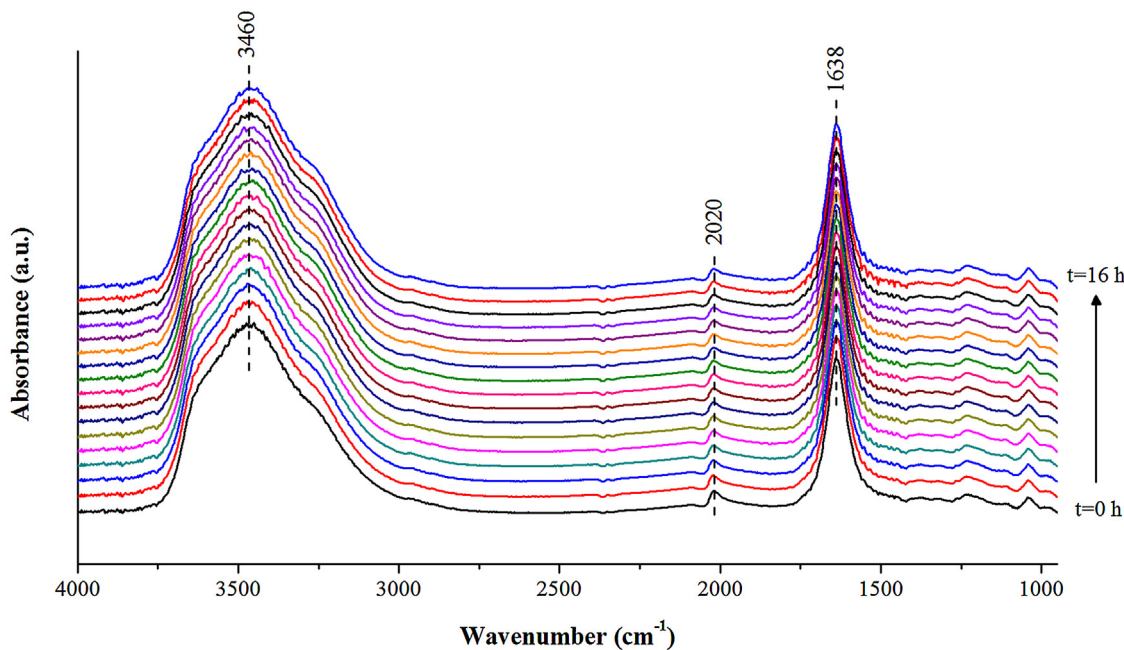


Fig. 1. Time-resolved *in-situ* ATR-IR spectra during the hydrogenolysis of 5 wt% glycerol in water over 9Pt8WAI at 200 °C and 45 bar of H₂.

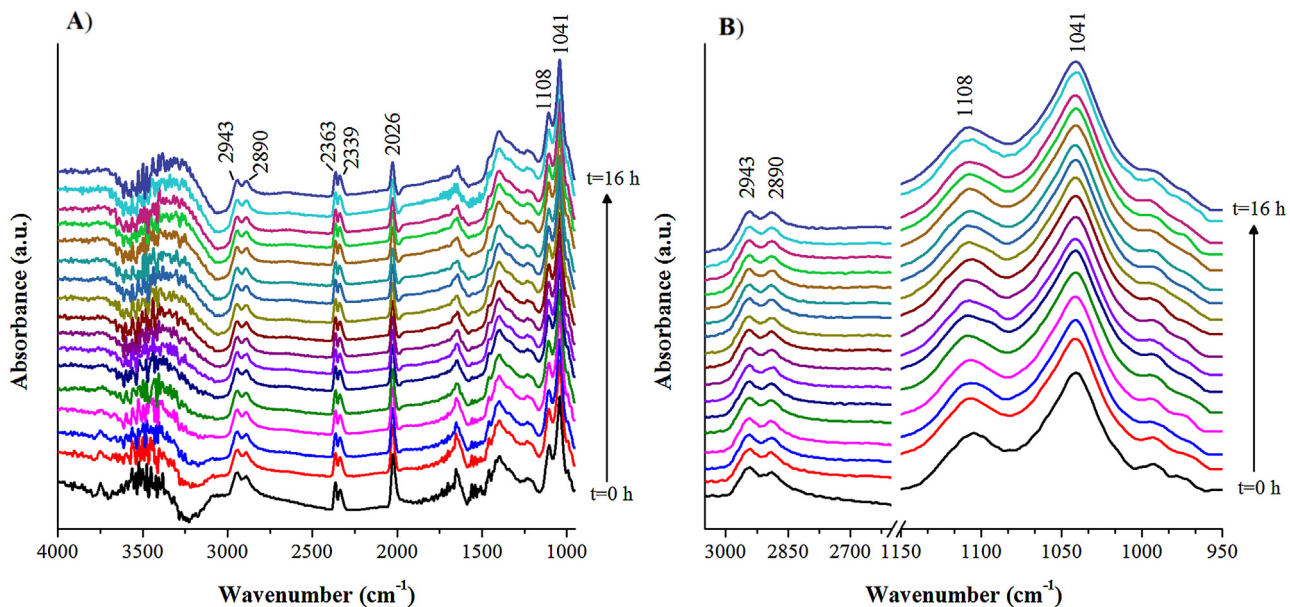


Fig. 2. Time-resolved *in-situ* ATR-IR spectra during the hydrogenolysis of 5 wt% glycerol in water over 9Pt8WAI at 200 °C and 45 bar of H₂ after water spectrum subtraction in the complete investigated region (A), and in the $\nu(\text{CH})$, 3000–2700 cm⁻¹, and $\nu(\text{CO})$, 1150–950 cm⁻¹, regions (B).

sure difference and by circulating a continuous flow of H₂ (or N₂) from the feed cylinder to the reactor for about 5 min. Thereafter, the pressure was increased up to the 45 bar.

After 16 h of reaction, the reactor was cooled down (<40 °C) and the gas phase was collected in a gas bag and analyzed with a GC-TCD-FID equipped with a molecular sieve column (HP-MOLESIEVE, diameter 0.535 mm, length 30 m) and a capillary column (HP-PLOT/Q, diameter 0.320 mm, length 30 m). The liquid sample was analyzed using 1,4-butanediol (Sigma-Aldrich, 99.99%) as standard with a GC-TCD-FID (Agilent Technologies, 7890 A) equipped with a Meta-Wax capillary column (diameter 0.53 mm, length 30 m).

The glycerol conversion and the selectivity towards liquid products were calculated based on the following Eqs. (1) and (2):

$$\text{Glycerol conversion (\%)} = \sum \frac{C\text{-based mol of all liquid product}_{t=t}}{C\text{-based mol of glycerol}_{t=0}} \times 100 \quad (1)$$

$$\text{Product selectivity (\%)} = \frac{C\text{-based mol of the product}_{t=t}}{\sum C\text{-based mol of all products}_{t=t}} \times 100 \quad (2)$$

3. Results

3.1. In-situ ATR-IR studies of glycerol hydrogenolysis

Time-resolved ATR-IR spectra of the surface species adsorbed on the 9Pt8WAI catalyst during the hydrogenolysis of a 5 wt% aqueous glycerol solution, at 200 °C and 45 bar of H₂, are shown in Fig. 1. In order to minimize the contribution of any possible modification of the catalyst layer, as well as the expansion of the IRE with the temperature, the spectrum of the catalyst layer coated on the IRE, and measured at the reaction temperature (200 °C), was used as the background.

Two strong absorption peaks characteristic of liquid water can clearly be observed: a very broad peak around 3460 cm⁻¹, which corresponds to the O–H stretching ($\nu(OH)$) mode and a peak at 1638 cm⁻¹ corresponding to the H–O–H scissor bending mode of water [29,30].

It is particularly important to highlight that there are no evidences for the hydration of the γ -Al₂O₃ support into boehmite (γ -AlO(OH)) during catalytic reaction, usually evidenced by the presence of a sharp peak at 1064 cm⁻¹ assigned to the OH deformation modes and shoulder bands at 3304, and 3124 cm⁻¹ to the stretching vibrational modes [31]. It was reported that the presence of both Pt and glycerol retards this transformation [31,32].

Interestingly, a peak centered at \sim 2020 cm⁻¹ with a shoulder at 1988 cm⁻¹ was detected. It was also observed in the blank-experiment with water under the same reaction conditions (not shown) and, therefore, it cannot be ascribed to the formation of CO during the reaction, which is expected to appear in this region [26,33]. In the work carried out by Ortiz-Hernández et al. they observed two peaks in the same region (a peak centered at 2060 cm⁻¹ and a shoulder at 1990 cm⁻¹) exposing a Pt/Al₂O₃ catalyst to a H₂ flow in water [34]. In their work, they demonstrated that those peaks were likely trace amounts of CO or other carbonyl species formed from impurities on the catalyst layer.

Unfortunately, the strong absorption of mid-IR by water may hinder the observation of other bands related to the intermediates or product species. In order to eliminate the contribution of the adsorbed water, the water spectrum (blank-experiment) was subtracted from the time-resolved spectra. The resulted spectra in the 4000–950 cm⁻¹ region are shown in Fig. 2A.

First of all, it is necessary to highlight the difficulty to identify the adsorbed species, since most of the compounds were alcohols and showed absorption bands at similar frequencies. Moreover, because of the strong absorbance of water in the 3600–3000 cm⁻¹ region, and the noise that the spectra contained after water subtraction, the $\nu(OH)$ mode of the reactant or the product species containing OH groups cannot be resolved. The large noise that also appeared in the region around 1870–1450 cm⁻¹ may also hinder other bands. This could be the case of the $\nu(C=O)$ characteristic modes of some potential intermediates, such as aldehydes (1740–1720 cm⁻¹), ketones (1725–1705 cm⁻¹) and acids (1725–1700 cm⁻¹) [35]. The peaks in the 2400–2000 cm⁻¹ region may correspond to some carbonyl species coming from impurities in the catalyst layer, as mentioned before: the peaks at 2363 and 2339 cm⁻¹ may be assigned to the adsorbed CO₂ [36] and the peak around 2026 cm⁻¹ to the linearly adsorbed CO [26].

Since the strongest and more defined bands were observed in the $\nu(CH)$, 3000–2700 cm⁻¹, and $\nu(CO)$, 1150–950 cm⁻¹, regions those regions are represented in Fig. 2B in more detail. The peaks around 2943 and 2890 cm⁻¹ can be ascribed to the asymmetric and symmetric stretching modes of the CH₂ group of glycerol, respectively (ν_{asym} and $\nu_{sym}(CH_2)$). Two additional peaks at 1108 and 1041 cm⁻¹ were also detected, which correspond to the $\nu(CO)$ of the 2° and of the 1° OH groups of glycerol [37]. Weaker defor-

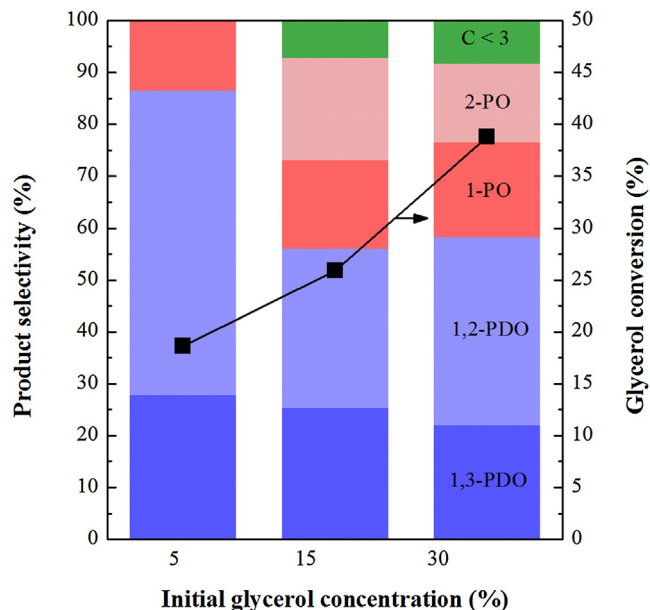


Fig. 3. Effect of initial glycerol concentration on the glycerol hydrogenolysis over 9Pt8WAI at 200 °C, 45 bar of H₂ and 16 h reaction time. C < 3: EG, ethanol and methanol.

mation modes likely associated with glycerol can be seen in the 1400–1200 cm⁻¹ region (see Fig. 2A).

The quite low glycerol conversion achieved (18.6%) after 16 h of reaction might be one of the reasons for which qualitative changes cannot be observed: neither the presence of species different from glycerol nor significant changes in the glycerol peak height. Thus, in order to increase the conversion of glycerol and to reduce the strong adsorption of water on the catalyst surface, two experiments were carried out with higher initial glycerol concentrations (15 and 30 wt%). Fig. 3 shows the effect of glycerol concentration on the glycerol hydrogenolysis over the 9Pt8WAI catalyst under the same reaction conditions (200 °C, 45 bar of H₂ and 16 h of reaction time).

According to the results, the glycerol conversion notably increased from 18.6 to 38.8% as its initial concentration in water was incremented from 5 to 30 wt%. Regarding the product selectivities, the most remarkable fact was the decrease in the selectivity towards 1,2-PDO. It decreased from 58.7% for 5 wt% of glycerol to 30.6% for 15 wt% and remained almost constant for higher glycerol concentrations. The selectivity towards 1,3-PDO slightly decreased as the glycerol concentration increased (from 27.8 to 22.0%, for 5 and 30 wt% glycerol). The downward trend of PDO selectivities could be explained by their over-hydrogenolysis mainly in favor of 1-PO, but also of 2-PO and the C–C hydrogenolysis reactions to some cracking products (C < 3), such as ethylene glycol (EG), ethanol and methanol.

For a deeper analysis, the water spectrum was subtracted from the time-resolved spectra of the hydrogenolysis of 15 wt% of glycerol. Fig. 4A shows the $\nu(CH)$ and the $\nu(CO)$ regions of those spectra. The same glycerol-related modes as those found in the hydrogenolysis of 5 wt% glycerol (Fig. 2B) were detected. All glycerol-related peaks became weaker as the reaction time increased. This can be clearly seen in the 2° $\nu(CO)$ mode at 1108 cm⁻¹, which almost disappeared after 3 h of reaction time. Higher initial concentration of glycerol led to a higher glycerol conversion and, therefore, to a larger formation of the reaction products. It should be expected that these products compete with glycerol for the active sites of the catalyst. Therefore, the question arises is why the peaks characteristic of the main products were not observed in the time-resolved spectra of Fig. 4A. Sievers et al. found that the polyols with more OH groups

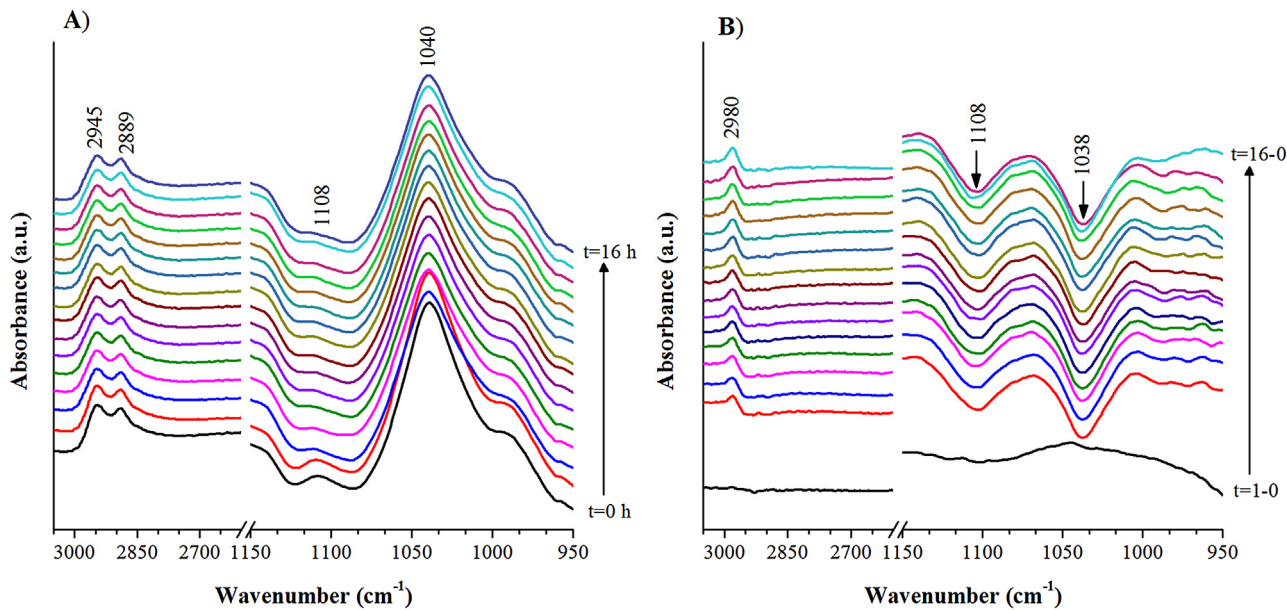


Fig. 4. Time-resolved *in-situ* ATR-IR spectra during the hydrogenolysis of 15 wt% glycerol in water over 9Pt8WAI (at 200 °C and 45 bar of H₂) after subtraction of water spectrum (A), and spectrum at *t* = 0 (B).

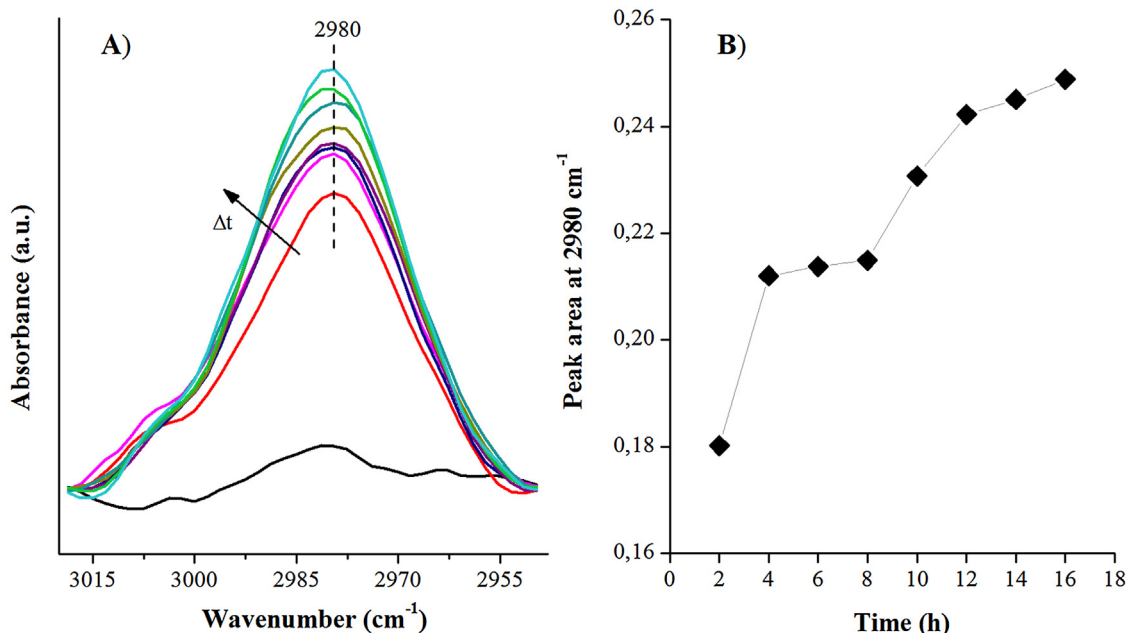


Fig. 5. The positive peak at 2980 cm⁻¹ developed in time (A), and the peak area evolution (B) during the hydrogenolysis of 15 wt% glycerol in water over 9Pt8WAI at 200 °C and 45 bar of H₂. Spectrum at *t* = 0 subtracted.

have stronger surface interactions on γ -Al₂O₃ and a higher uptake from the aqueous solutions than those with fewer OH groups [37]. In our measurements glycerol was present in greater concentrations, which also explains why glycerol was detected more clearly than any other reaction product under the operating conditions used.

In order to overcome the strong signal of glycerol, the spectrum at initial time (*t* = 0) was subtracted from the time-evolution spectra of the hydrogenolysis of 15 wt% aqueous glycerol. As observed in Fig. 4B, at *t* = 0 glycerol is considered to be the unique compound adsorbed, excluding water, on the catalyst surface. At *t* > 0 two strong negative peaks appeared at 1108 and 1038 cm⁻¹ associated with the ν (CO) modes of glycerol. They revealed the lower

adsorption of glycerol because of the competitive adsorption with the products formed along the reaction.

Very interestingly, a positive clearly defined peak appeared at 2980 cm⁻¹, whose area increased as the reaction moved forward, as it can be observed in more detail in Fig. 5. The appearance of positive peaks suggests the progressive adsorption of one or more reaction products on the catalyst surface along the reaction. It is reasonable to qualitatively correlate the peak integrated-area to the extent of a product formation.

The analysis of the ATR-IR spectra of the hydrogenolysis of 30 wt% aqueous glycerol, after the spectrum at *t* = 0 was subtracted, provided more information about the origin of the band around 2980 cm⁻¹. Fig. 6 shows the ν (CH) region of those spectra. A band at

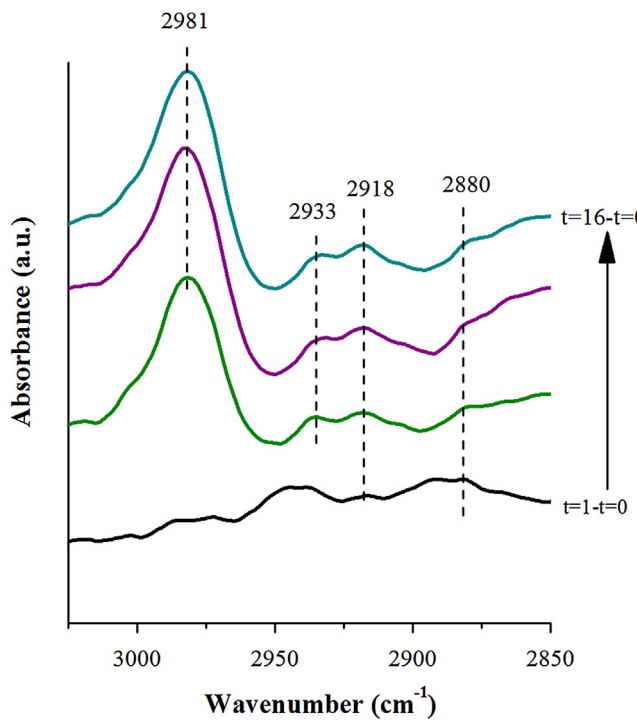


Fig. 6. Time-resolved *in-situ* ATR-IR spectra during the hydrogenolysis of 30 wt% glycerol on water over 9Pt8WAI at 200 °C and 45 bar of H₂, after spectrum at t=0 was subtracted, in the $\nu(\text{CH})$ region.

a similar position, 2981 cm⁻¹, and other two at 2933 and 2880 cm⁻¹ were found, which may be ascribed to the $\nu_{\text{asym}}(\text{CH}_3)$, $\nu_{\text{asym}}(\text{CH}_2)$ and $\nu_{\text{sym}}(\text{CH}_2)$ of 1,2-PDO, respectively [37].

Despite the fact that the surface species formed by other product species, such as 1-PO, 2-PO or ethanol, also exhibit $\nu(\text{CH}_3)$ and $\nu(\text{CH}_2)$ bands with nearly identical frequencies [38–40], it is reasonable to think that they could correspond to 1,2-PDO, since it is the major product in the reaction (30.6 and 36.1% selectivity for the experiments with 15 and 30 wt% initial glycerol concentrations). In addition, the higher number of OH groups of 1,2-PDO makes its adsorption on the catalyst surface easier [37], as it was explained above. The preliminary kinetic studies carried out in the current work (see Section 3.3) shed more light on the matter and support this hypothesis. Obviously, the assignment of those peaks to 1,3-PDO can be ruled out since this compound does not show the $\nu(\text{CH}_3)$ mode.

Another peak centered at 2918 cm⁻¹ was observed and likely corresponds to the $\nu_{\text{asym}}(\text{CH}_2)$ characteristic group [41]. The position of this IR peak is quite far from the absorption bands of the bulk species (when they are not adsorbed), the products analyzed by GC-TCD-FID (PDO, 1-PO, EG or ethanol), the main intermediates involved in the reaction, acetol and propanal (detected in other experiments performed, see Section 3.4), and other suggested intermediates, such as acrolein [30,35]. Nevertheless, the formation of an adsorbed alkoxide coming from some of these compounds could shift the band position or originate a new band.

3.2. Ex-situ ATR-IR studies of glycerol hydrogenolysis

The ATR-IR spectroscopy working is not limited to *in-situ* measurements. Indeed, it is also very useful for obtaining ATR-IR spectra of samples that cannot be readily examined by common transmission methods, such as thick or highly absorbing solids and liquid samples [41]. In this work, *ex-situ* ATR-IR spectroscopy was used to study the interactions of glycerol as reactant with different catalyst

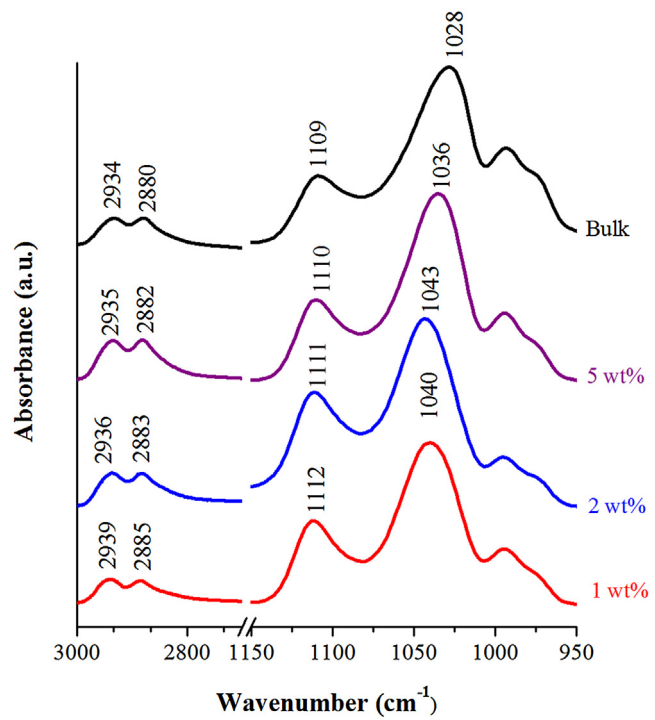


Fig. 7. *Ex-situ* ATR-IR spectra of the different glycerol loadings (1–5 wt%) on Al support after the removal of water by high vacuum, and the spectra of the bulk pure glycerol directly deposited on the ZnSe IRE (bulk).

surfaces (*i.e.*, Al and 8WAI) and establish the role of the tungsten oxide in the glycerol-anchoring step.

For this purpose, a layer of alumina support was immobilized on the IRE (details in Section 2.2) and its spectrum was used as background. It was then impregnated with different glycerol aqueous solutions: 0.5, 1.0, 2.0 and 5.0 wt% of glycerol. Their different spectra are shown in Fig. 7. The weak IR signals obtained in the 0.5 wt% loading test did not allow clear peak discrimination and, therefore, those results were not included. In these experiments, after glycerol was loaded on the sample, the bulk water was removed by applying high vacuum (HV). Thereby, the interactions between glycerol and the catalyst surface, but also bulk glycerol signals can be observed. The existence of those reactant-surface interactions is demonstrated by the changes in the glycerol $\nu(\text{CH})$ and especially in the $\nu(\text{CO})$ modes compared to those of bulk pure glycerol (directly loaded on the IRE).

As the concentration of glycerol in the solution used to impregnate the alumina material increased, the spectra became more similar to the bulk glycerol. The reason for this is that not only the signals from adsorbed glycerol molecules, but also the signals from the bulk molecules, just deposited on the surface, are increasingly more perceptible [37].

The 2° $\nu(\text{CO})$ was positioned at 1112 cm⁻¹ for the Al support impregnated with 1 wt% glycerol, and shifted to lower wavenumbers as the concentration of the aqueous solutions increased. It should be noted that a more remarkable change was observed for the 1° $\nu(\text{CO})$ mode, which changed from 1040 cm⁻¹ for 1 wt% to 1028 cm⁻¹ for the bulk pure glycerol spectra, meaning a significant shift of 12 cm⁻¹. It indicates that the surface interactions between the 1° OH group/s of glycerol are stronger than those of the 2° OH group. Small changes were noted for the $\nu(\text{CH}_2)$ modes: the $\nu_{\text{asym}}(\text{CH}_2)$ and $\nu_{\text{sym}}(\text{CH}_2)$ modes changed from 2939 and 2885 cm⁻¹ for 1 wt% of glycerol to 2934 and 2880 cm⁻¹ for the bulk pure glycerol, respectively.

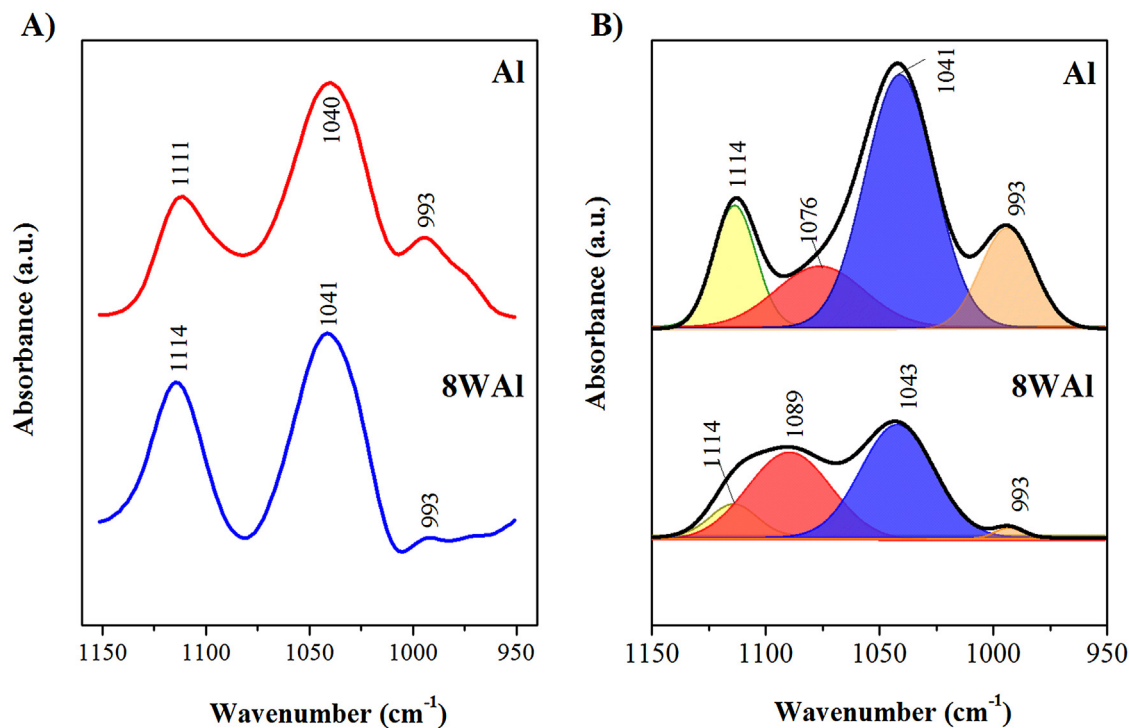


Fig. 8. Comparison of the ATR-IR spectra of 1 wt% glycerol in water loaded on Al and 8WAl, after the removal of water by high-vacuum (A), and after the water spectrum was subtracted from the glycerol loaded sample (B).

Despite that the interactions found in the current study are not as strong as in other works [37], the shifts indicate that the electronic structure of glycerol slightly changed and, therefore, a physisorbed or weakly chemisorbed glycerol is formed on the catalyst surface. Moreover, our experiments cannot rule out the formation of a stronger alkoxide under real reaction conditions.

The loading, which maximized the ratio between the signal from the adsorbed glycerol and those from the bulk glycerol, was 1 wt%. Thus, this was the selected loading to study the role of the tungsten oxides in the adsorption step of glycerol. The effect of the incorporation of Pt was not studied in the present work, since its role in the hydrogenolysis reaction is quite well-established; namely to activate the hydrogen molecules [42].

It is necessary to point out that the HV, which is used to remove the water from the impregnated samples, could also modify the surface of the catalyst materials and as a consequence of this the glycerol-active sites interactions. In order to verify this hypothesis, the spectrum of the samples with water was subtracted from the spectrum of the samples loaded with aqueous glycerol (denoted as WS, water subtraction). Then, they were compared with the spectra of the samples treated with HV. The $\nu(\text{CO})$ regions ($1150\text{--}950\text{ cm}^{-1}$) of 1 wt% glycerol loaded on the Al support, as well as on the tungstated alumina (8WAl) are represented in Fig. 8. With the HV treatment, the glycerol $\nu(\text{CO})$ vibrational modes appeared at lower wavenumbers (Fig. 8A) than those samples, which did not undergo that treatment, WS (Fig. 8B). Moreover, some glycerol absorption bands were also hidden. These facts verify the previous hypothesis and show that HV is not the proper treatment.

Comparing the WS spectra, it is interesting to highlight that very remarkable differences are detected in the spectrum shapes and the band positions between the glycerol adsorption on Al and 8WAl. The shift in the IR frequency is a complex matter; it could include the change in the dipole moment of the adsorbed molecule or small steric and electronic effects [43,44]. In spite that the nature of those shifts remains unclear, the very different spectra suggest, at least, a different interaction between glycerol and the catalyst surface

when tungsten oxides are incorporated on the $\gamma\text{-Al}_2\text{O}_3$ support. However, both support oxides have something in common: the glycerol seems to be adsorbed by the terminal OH group/s, since this mode undergoes the highest shift related to the vibrational modes of bulk glycerol ($\Delta\nu = 13\text{--}15\text{ cm}^{-1}$). The different strength of interaction is highlighted in the $\nu(\text{CO})$ mode region: the $1^\circ \nu(\text{CO})$ band became weaker and a new broad band at 1089 cm^{-1} appeared when glycerol is adsorbed on the 8WAl sample, whereas the $2^\circ \nu(\text{CO})$ remained at the same position, i.e., 1114 cm^{-1} . This fact suggests a stronger interaction between the 1° OH group/s of glycerol when tungsten oxides are present over the $\gamma\text{-Al}_2\text{O}_3$. Thus, the formation of a glycerol alkoxide is suggested over the tungsten oxides.

3.3. Glycerol and products competition for the same active sites

Kinetic measurements are often used to provide important information about the reaction mechanism of a catalytic process [45]. In the present work, a preliminary kinetic study was performed in order to determine whether the main reaction products of the glycerol hydrogenolysis compete with glycerol as reactant for the same active sites of the catalyst, as the *in-situ* ATR-IR spectroscopy results seem to indicate.

For those experiments, all the reaction parameters, temperature, pressure, and stirring speed, were held constant (conditions and experimental details available in Section 2.5). Different aqueous feed solutions were introduced into the reactor: (a) 5 wt% glycerol, and (b) 1,2-PDO, (c) 1,3-PDO and (d) 1-PO together with 5 wt% glycerol (product to glycerol molar ratio of 1).

Based on the glycerol conversion results, shown in Fig. 9, it is clear that glycerol reaction rate was affected when the three products were used as reactants. The decrease of the glycerol reaction rate is due to the competition of products and glycerol for the same active sites. The PDO, in particular, had a more remarkable effect on the decrease of the glycerol conversion: 1,2-PDO reduced it from 11.6% to 3.7%, and, 1,3-PDO even to a lower value of 2.8%, whereas 1-PO decreased the conversion to a lesser extent (6.7%).

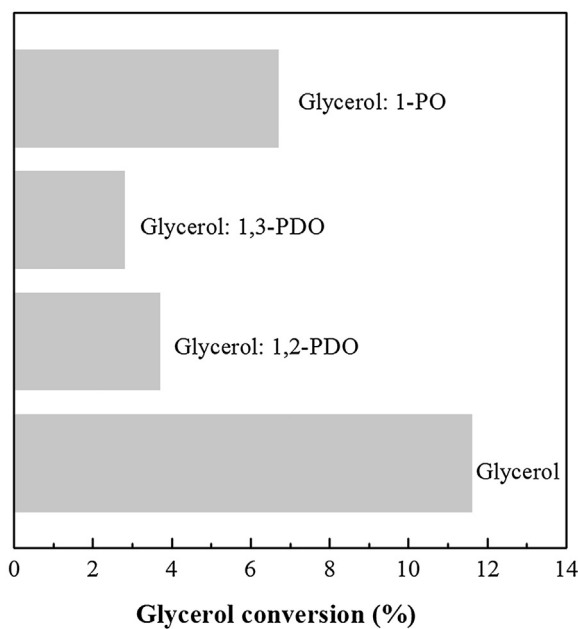


Fig. 9. Glycerol conversion values achieved in the hydrogenolysis reaction using different reactants at 200 °C, 45 bar H₂ and 2 h of reaction time. Concentration of glycerol in water = 5 wt%. Glycerol: product molar ratio of 1:1.

As described before, the number of OH groups has a great importance on the adsorption, since the possibilities for a molecule to be adsorbed usually increase with the number of those groups in the chain [37]. It adds one more reason to confirm that 1,2-PDO was the adsorbed molecule most likely detected in the *in-situ* ATR-IR spectroscopy experiments with 15 and 30 wt% glycerol, after spectra at t = 0 was subtracted (see Figs. 5 and 6), instead of any other monoalcohol, like 1-PO.

However, according to the work of Bronswijk et al., the adsorption affinities of polyols increased with the increasing number of vicinal OH groups present in the chain [46]. This is not the case for the current study since the adsorption seems to be greater for 1,3-PDO than for 1,2-PDO. According to the *ex-situ* ATR-IR spectroscopy findings, glycerol was adsorbed by the terminal OH group/s. Therefore, it could be expected, that the adsorption of PDO occurred preferentially by the same functional groups. The greater adsorption of 1,3-PDO, which exhibit two terminal OH groups, than 1,2-PDO, of only one, is in good agreement with this adsorption trend.

In view of this result, it is not clear why the more strongly adsorbed 1,3-PDO was not detected in the *in-situ* ATR-IR measurements, unlike the adsorbed 1,2-PDO. The reason could lie in the fact that 1,3-PDO and glycerol exhibit bands at similar frequencies in the $\nu(\text{CH})$ region [30] which cancel out each other, since those attributed to the product formation were positive and those of reactant consumption negative, after spectra at t = 0 was subtracted. Moreover, the broad negative bands of glycerol in the $\nu(\text{CO})$ region made it impossible to differentiate between any of the peaks in this spectral region.

3.4. Effect of the reacting atmosphere and the hydrogen availability

The hydrogenolysis of glycerol, 1,2-PDO and 1,3-PDO (5 wt% in water) was carried out over 9Pt8WAl catalyst under both H₂ and N₂ atmospheres. The catalytic activity test results are detailed in Table 2.

The most frequently proposed mechanism in the literature is the dehydration-hydrogenation route [47,48], in which glycerol is first

dehydrated to acetol or 3-HPA and further hydrogenated to 1,2-PDO or 1,3-PDO, respectively. Trace amounts of acetol were found in the glycerol hydrogenolysis under H₂ atmosphere, whereas the presence of 3-HPA was not detected. The acetol formation is thermodynamically more favored than that of 3-HPA [49,50] and, therefore, 1,2-PDO is usually the major product among PDO. However, in this case, the selectivity towards 1,3-PDO (38.5%) was much higher than that towards 1,2-PDO (9.0%). This fact could arise from two factors: (i) a different reaction mechanism was involved or, (ii) 1,2-PDO was more reactive than 1,3-PDO.

However, under H₂ pressure both PDO showed similar reactivity (see Table 2) indicating a higher formation of 1,3-PDO during the glycerol hydrogenolysis. It is worth noting that the overhydrogenolysis to 1-PO was the main reaction involved in the PDO conversion. This explains quite well why 1-PO was formed in high quantities when glycerol is used as reactant (36.9% selectivity). It is important to highlight that the molar ratio 1-PO/2-PO obtained from 1,2-PDO (*i.e.* 4.6) is similar to the 1,3-PDO/1,2-PDO ratio obtained from glycerol (*i.e.* 4.3). This fact suggests that the conversion of 1,2-PDO follows the same reaction mechanism than glycerol.

The same experiments were performed under N₂ pressure in order to investigate the effect of the reacting atmosphere and the hydrogen availability. The glycerol conversion value under N₂ atmosphere (22.2%) was extremely low compared to that under H₂ (80.3%). This result seems to indicate that hydrogen plays an important role in the activation of glycerol. Moreover, the lower availability of hydrogen also affected the product distribution: 1,2-PDO and acetol (57.3 and 21.4% selectivities) were the major products. Since the hydrogenation of acetol to glycerol consumed hydrogen, and it was not externally provided, it should be *in-situ* generated by aqueous phase reforming (APR) reactions of glycerol [51,52]. The APR of glycerol is a well-known process; the reaction stoichiometry is shown in the Eq. (3).



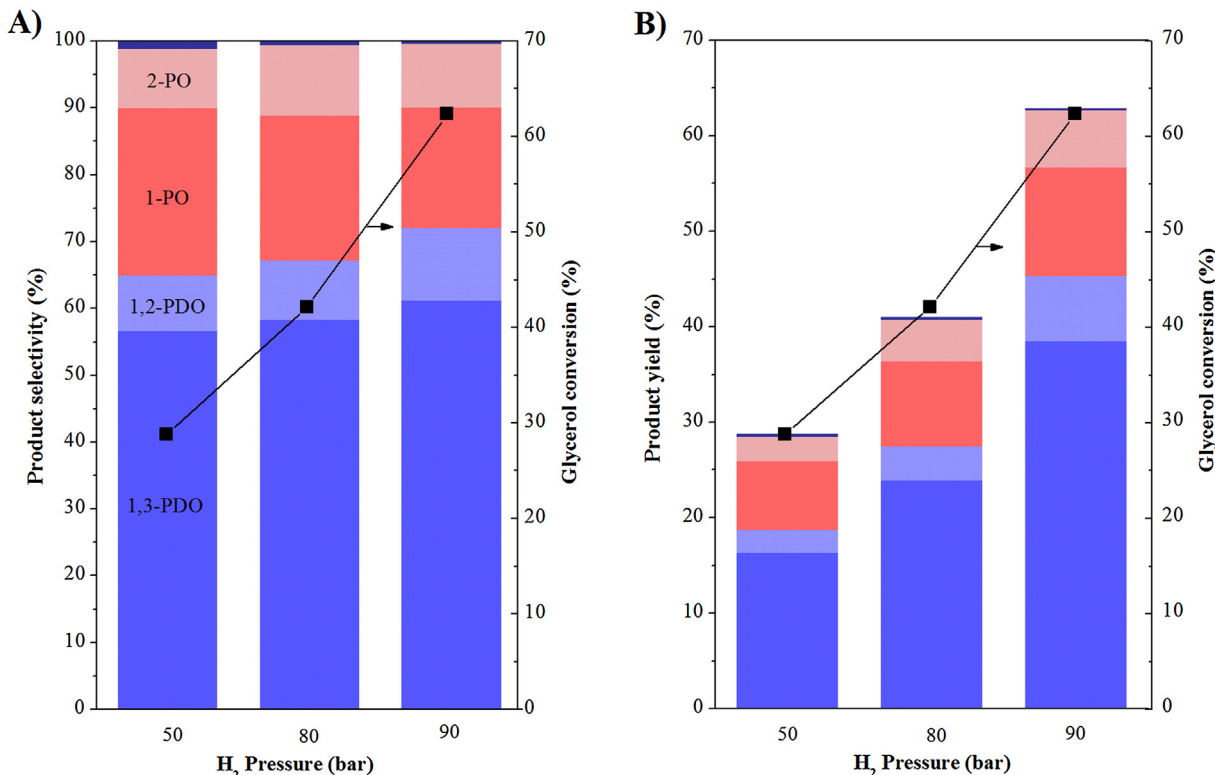
However, neither 1,3-PDO nor 2-PO (or acetone) products were detected in the hydrogenolysis of glycerol under inert N₂. This is an interesting fact that reveals that the high availability of hydrogen is necessary for the glycerol conversion into those products.

Unexpectedly, when 1,3-PDO was used as reactant, a higher conversion under N₂ than under H₂ atmosphere was found (*i.e.*, 46.4% under N₂ and 23.9% under H₂). These results reveal the instability of 1,3-PDO under low hydrogen availability conditions. Unlike 1,3-PDO, the conversion of 1,2-PDO under N₂ was lower than that obtained under H₂.

In order to determine the influence of the H₂ pressure, the glycerol hydrogenolysis reaction was carried out at 50, 80 and 90 bar over the 9Pt8WAl catalyst. For this study a higher concentration of glycerol (20 wt% in water) nearer to the real feed concentration, which is obtained during the biodiesel manufacture, was used. As it can be observed in Fig. 10, the increase of the pressure provided a positive effect on the glycerol conversion, which might be due to the increase in the concentration of protons and hydride ions formed from the hydrogen, which are involved in the activation of glycerol molecules [53]. The increase of the glycerol conversion was accompanied by a slight increase in the selectivity towards 1,3-PDO, which is translated into a higher yield of this product. The highest yield of 1,3-PDO (38.5%) was obtained at 90 bar of H₂ pressure at only 4 h of reaction time (Fig. 10B). Interestingly, the selectivity towards 1-PO decreased with the initial H₂ pressure increase. This could be explained by the higher stability of the 1,3-PDO compound as hydrogen molecules are more readily available.

Table 2Catalytic activity test results of the hydrogenolysis of glycerol and propanediols under H_2 atmosphere at 220 °C, 45 bar and 16 h of reaction time.

Atm.	Reactant	Conv. (%)	Selectivity towards liquid products (%)								
			1,3-PDO	1,2-PDO	1-PO	2-PO	Acetol	Acetone	Propanal	Prop. acid	Ethanol
H_2	Glycerol	80.3	38.5	9.0	36.9	7.2	*	3.1	0.0	*	3.9
	1,3-PDO	23.9	–	0.0	80.8	0.0	0.0	0.0	0.0	2.3	7.9
	1,2-PDO	26.6	0.0	–	70.8	15.5	0.0	5.1	0.0	0.0	0.0
N_2	Glycerol	22.2	0.0	57.3	7.3	0.0	21.4	0.0	0.0	0.0	5.9
	1,3-PDO	46.4	–	0.0	42.2	0.0	0.0	0.0	2.1	4.2	6.8
	1,2-PDO	13.8	0.0	–	29.7	0.0	22.7	6.2	0.0	0.0	17.8

**Fig. 10.** Influence of the H_2 pressure on the glycerol conversion and product selectivities (A) and product yields (B) obtained during the glycerol hydrogenolysis over 9Pt8WAI at 200 °C and 4 h of reaction time.

4. Discussion

The main goal of this research work is to analyze the role of the tungsten oxide on the selective glycerol hydrogenolysis to 1,3-PDO. The evidences found in this regard lead to a better understanding of the reaction pathways and some of their fundamental aspects.

In our previous findings [22], it was reported that the tungsten surface density was the parameter that controls the type of tungsten oxide species present on the catalyst surface. They may be present as: monotungstates (WO_4), polytungstates (WO_5/WO_6) and WO_3 nanoparticles (NPs) [54,55]. The highest yield of 1,3-PDO was obtained at a tungsten surface density of 2.4 W at. nm⁻². For this value, the largest Brønsted to Lewis ratio was obtained, due to the highest concentration of polytungstates without the appearance of NPs. The 9Pt8WAI catalyst employed in the present work shows a similar tungsten surface density value (i.e. 2.2 W at. nm⁻²), which ensures that its surface is mainly composed of highly dispersed polytungstate species.

The necessity of Brønsted acidity for the production of 1,3-PDO was widely proven in the literature [53,56,57]. In fact, some reports attributed to the tungsten oxide the unique role of acting as a Brønsted acidity supplier [58–60]. Interestingly, the findings obtained in this work through the *ex-situ* ATR-IR spectroscopy (Section 3.2)

broaden the information about the different roles of the tungsten oxide on the glycerol hydrogenolysis (see Fig. 11, mechanism A). According to these observations, the tungsten oxide acid sites are also involved in the hydrogenolysis of glycerol to 1,3-PDO by anchoring the 1° OH group/s of glycerol and forming a strongly bonded terminal alkoxide. The formation of similar alkoxides over a Rh- and Ir-ReO_x/SiO₂ catalysts were previously proposed by the Tomishigue's group [12,19,61,62], but its formation was not experimentally evidenced until this report. Despite the authors of this previous study explained their high selectivities towards 1,3-PDO because of the preferential terminal alkoxide formation on the ReO_x, we found that the glycerol is adsorbed by the terminal OH group/s regardless of the presence of the oxophilic metal (over Al or 8WAI).

As it was previously suggested [22], a proton coming from a Brønsted acid site of the tungsten oxide, provided by polytungstate species, protonates the internal OH group of glycerol (the 2°) which possesses the highest proton affinity [63]. Polytungstates, unlike the other tungsten species, form an extended network of tungsten oxides which have the ability to undergo a slight reduction by delocalizing the net negative charge over several tungsten atoms and accommodate the protons coming from the hydrogen dissociation [55,64]. After dehydration a 2° carbocation is formed.

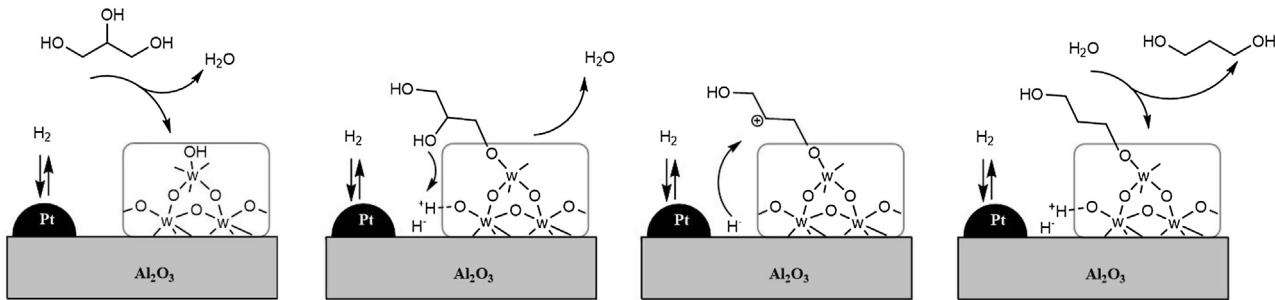


Fig. 11. Mechanism A: reaction mechanism proposed for the glycerol hydrogenolysis to 1,3-PDO (modified from ref. [22]).

The carbocation is then attacked by a hydride species coming from the heterolytic activation of molecular hydrogen on the Pt active sites [53,65]. At this point, the stabilization and the fast hydrogenation of the 2° carbocation are of vital importance. The polytungstate species present on the catalyst take part in its stabilization by delocalizing the negative charge. The stronger adsorption over those species rather than on the Al support, according to the *ex-situ* ATR-IR experiments, may also be involved in the 2° carbocation stabilization avoiding the releasing of the alkoxide before the hydride attack. It could lead to the formation of acrolein, the precursor of 1-PO.

Furthermore, according to the results obtained under H₂ and N₂ reacting atmospheres (Section 3.4), the high availability of hydrogen and, therefore, hydride ions is indispensable in order to produce 1,3-PDO from glycerol. The experiments carried out at different H₂ pressures (Fig. 10) are in agreement with this hypothesis. The best results were obtained at 90 bar of H₂ pressure at only 4 h of reaction time using a glycerol concentration of 20 wt% (38.5% yield of 1,3-PDO). After the hydride attack, the hydrolysis of the alkoxide yields the 1,3-PDO compound. The importance of the availability of hydrogen was also demonstrated in the glycerol hydrogenolysis under N₂ atmosphere, in which 1,3-PDO was not detected and 1,2-PDO was obtained as the main product, instead. Moreover, the hydrogenolysis of 1,3-PDO under N₂ atmosphere revealed the high instability of this compound when hydrogen is not readily available, favoring the APR and cracking reactions. It should be added that despite hydrogen molecules were formed during the hydrogenolysis of glycerol under N₂ atmosphere, their concentration was not high enough to produce 1,3-PDO.

Thus, the evidences obtained in this work about the role of the oxophilic metal on the glycerol hydrogenolysis to 1,3-PDO can be summed up in a triple-action of the supported tungsten oxide: (1) it acts as a strong anchoring site for the 1° OH group/s of glycerol forming a terminal alkoxide, (2) it provides the necessary Brønsted acid sites to protonate the internal OH group of glycerol, and (3) it stabilizes the 2° carbocation formed, avoiding the degradation of the 1,3-PDO product.

According to the activity test results under H₂ atmosphere, a different reaction mechanism for the formation of 1,2-PDO should be involved, in which the Lewis acid sites, mainly of the γ-Al₂O₃, may be implicated (mechanism B, see Fig. 12). The interaction of glycerol with Lewis acid sites is affected by steric constrains [66], in contrast to the glycerol protonation discussed above. According to this scheme, the terminal OH group of glycerol is more likely to interact with the Lewis acid sites, which was also found in the *ex-situ* ATR-IR measurements. The migration of the proton of the 2° carbon to the oxygen of the Lewis site could release 2,3-dihydroxypropene which further suffer a keto-enol tautomerization to yield acetol. The hydrogenation of acetol released the 1,2-PDO.

As it can be observed in Table 2 the reactivity trend for 9Pt8WAl catalysts was: glycerol>1,2-PDO (26.6%) ≈ 1,3-PDO (23.9%), which

differs from the reactivity trend reported previously [67]. However, as it is explained below, the observed trend completely matches with our proposed mechanisms. The results from *ex-situ* ATR-IR showed that glycerol is adsorbed on the catalyst surface through a primary hydroxy group. Therefore, it is reasonable that glycerol has a higher reactivity than 1,2-PDO as it presents two terminal hydroxy groups instead of one. As it was mentioned before, glycerol can react following the proposed mechanism A to form 1,3-PDO through an intermediary secondary carbocation, or following the mechanism B to form 1,2-PDO. Similarly, 1,2-PDO can react following the mechanism A to form 1-PO or following the mechanism B to 2-PO. With respect to the formation of 1,3-PDO, it has to be taken into account that it cannot react through mechanism A (adsorbed on tungsten oxide sites), because it does not have a secondary hydroxy group. Therefore, it is coherent that its reactivity is lower than the one of glycerol, because 1,3-PDO will only react on those active sites that catalyze the mechanism B (alumina sites).

Regarding the reactivity of both diols, it is worth mentioning that despite the fact that 1,3-PDO presents a higher tendency for adsorption than 1,2-PDO, because it has two terminal hydroxy groups instead of one, 1,2-PDO can react though both mechanisms. All things considered, both diols present a similar reactivity.

The proposed reaction mechanisms also explain why the conversion of glycerol remarkably decreased under N₂ atmosphere and why 1,3-PDO is not formed. Under N₂, only the fraction of glycerol adsorbed on the aluminum sites would react and mainly form 1,2-PDO. The fraction of glycerol adsorbed on the tungsten oxides cannot be activated since the hydrogen required for the protonation of the alkoxide, and the following hydride attack, is not available.

Additionally, this study shows the potential of *in-situ* ATR-IR spectroscopy as a powerful characterization tool for catalyst research since it could observe the changes that occur at a catalytic surface during reaction. It also allows characterizing adsorbed molecules on heterogeneous catalysts in liquids with very strong absorbance, such as water, for which the more conventional IR spectroscopies are not (very) suitable. Although the measurements in water are still very difficult to perform, as this work also highlighted, it was possible to measure in real time the changes in adsorbed molecules/surface catalyst interactions as the reactant was consumed and the products were formed (Section 3.1). Unfortunately, the similar nature of the majority of the reaction products obtained in the glycerol hydrogenolysis, added an extra difficulty to this work: the product identification was very hard since all of them showed absorption bands at similar frequencies. In spite of this, the *in-situ* ATR-IR spectroscopic measurements carried out in this work during the glycerol hydrogenolysis revealed the high competition for the same active sites between glycerol and PDO, as the kinetic measurements confirmed (Section 3.3). Moreover, the technique provided experimental evidence for the high thermal stability of the support, which remains as γ-Al₂O₃ during catalysis.

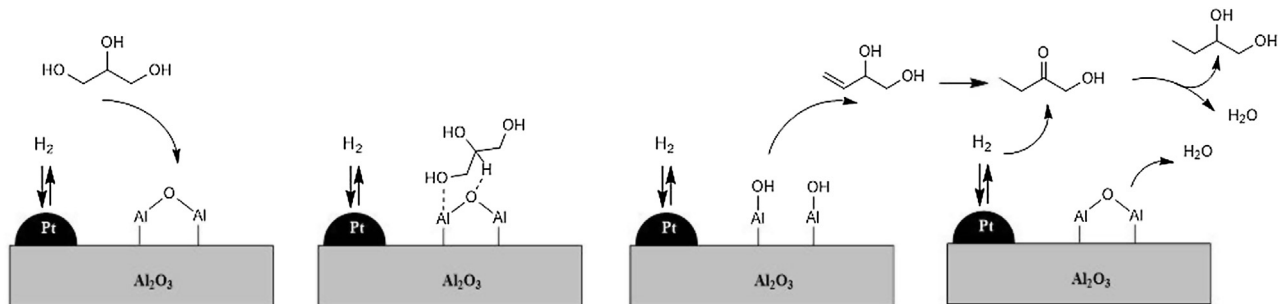


Fig. 12. Mechanism B: reaction mechanism proposed for the glycerol hydrogenolysis to 1,2-PDO.

5. Conclusions

In-situ ATR-IR spectroscopy was applied to the hydrogenolysis of glycerol over Pt/WO_x/Al₂O₃ catalysts demonstrating the high competition for the same catalytic active sites between glycerol and the reaction products 1,2-PDO and 1,3-PDO. ATR-IR spectroscopy turned to be a very useful characterization tool to investigate the catalytic solids in real time, and to reveal that the support γ -Al₂O₃ material was not hydrated into boehmite during the reaction, in spite of the hydrothermal conditions employed.

The application of *ex-situ* ATR-IR spectroscopy to the adsorption of glycerol aqueous solutions over the Al support and 8WAl catalyst provided new mechanistic information about the initial adsorption step. Despite the adsorption seems to occur through the terminal OH groups of glycerol over both aluminum and tungsten oxide sites, the adsorption strength seems to be stronger over the catalyst loaded with tungsten oxides. This could contribute to the stabilization of the 2° carbocation formed during the hydrogenolysis of glycerol, before it is subsequently hydrogenated and transformed into 1,3-PDO, the reaction product of interest.

The experiments carried out under N₂ atmosphere, in which hydrogen was not provided externally, revealed the necessity of high hydrogen availability in the medium. The high availability of Brønsted acid sites and the fast hydrogenation of the 2° carbocation seem to be the key parameters in order to boost the formation of 1,3-PDO. For all of this, it was suggested that the tungsten oxide plays three important roles, *i.e.*, (a) as anchoring site for the 1° OH group/s of glycerol, (b) as supplier of protons and (c) as stabilizer of the 2° carbocation formed. A notable high yield of 1,3-PDO of 38.5% was reported for the 9Pt8WAl catalyst material under study at 200 °C, 90 bar of H₂ and 4 h of reaction time.

Acknowledgments

This work was supported by University of the Basque Country (UPV/EHU), European Union through the European Regional Development Fund (ERDF) (Spanish MICIN Project: CTQ2015-64226-C3-2R), and the Basque Government (Researcher Training Program of the Department of Education, Universities and Research). The authors also gratefully acknowledge Dr. Pieter Bruijnincx (Utrecht University, UU) for the discussions on the ATR-IR data, Ana Hernández and Khaled Khalili (UU) for their technical support and Uxue Astobiza (UPV/EHU) for the activity measurements done in the frame of this research work. The authors also wish to express all their gratitude to Prof. Belén M. Güemez (UPV/EHU) for her dedication to science and related research work in the group SuPrEn.

References

- [1] J. Tendam, U. Hanefeld, Renewable chemicals: dehydroxylation of glycerol and polyols, *ChemSusChem* 4 (2011) 1017–1034.
- [2] M. Pagliaro, M. Rossi, *The Future of Glycerol: New Uses of a Versatile Raw Material*, 2nd ed., The Royal Society of Chemistry, Cambridge, 2008.
- [3] C.-H. Zhou, J.N. Beltramini, Y.-X. Fan, G.Q. Lu, Chemoselective catalytic conversion of glycerol as a biorenewable source to valuable commodity chemicals, *Chem. Soc. Rev.* 37 (2008) 527–549.
- [4] A. Corma Canos, S. Iborra, A. Velty, Chemical routes for the transformation of biomass into chemicals, *Chem. Rev.* 107 (2007) 2411–2502.
- [5] F. Dumeignil, A new concept of biorefinery comes into operation: the EuroBioRef concept, in: A. Michele, D. Angela, F. Dumeignil (Eds.), *Biorefinery From Biomass to Chem. Fuels*, 1st ed., De Gruyter, Berlin/Boston, 2012, pp. 1–17.
- [6] Y. Nakagawa, K. Tomishige, Heterogeneous catalysis of the glycerol hydrogenolysis, *Catal. Sci. Technol.* 1 (2011) 179–190.
- [7] I. Gandarias, J. Requies, P.L. Arias, U. Armbruster, A. Martin, Liquid-phase glycerol hydrogenolysis by formic acid over Ni-Cu/Al₂O₃ catalysts, *J. Catal.* 290 (2012) 79–89.
- [8] Z. Yuan, L. Wang, J. Wang, S. Xia, P. Chen, Z. Hou, X. Zheng, Hydrogenolysis of glycerol over homogeneously dispersed copper on solid base catalysts, *Appl. Catal. B Environ.* 101 (2011) 431–440.
- [9] Z. Yuan, P. Wu, J. Gao, X. Lu, Z. Hou, X. Zheng, Pt/solid-base: predominant catalyst for glycerol hydrogenolysis in a base-free aqueous solution, *Catal. Lett.* 130 (2009) 261–265.
- [10] J. Feng, J. Wang, Y. Zhou, H. Fu, H. Chen, X. Li, Effect of base additives on the selective hydrogenolysis of glycerol over Ru/TiO₂ Catalyst, *Chem. Lett.* 36 (2007) 1274–1275.
- [11] L. Huang, Y.-L. Zhu, H.-Y. Zheng, Y.-W. Li, Z.-Y. Zeng, Continuous production of 1,2-propanediol by the selective hydrogenolysis of solvent-free glycerol under mild conditions, *J. Chem. Technol. Biotechnol.* 83 (2008) 1670–1675.
- [12] Y. Shinmi, S. Koso, T. Kubota, Y. Nakagawa, K. Tomishige, Modification of Rh/SiO₂ catalyst for the hydrogenolysis of glycerol in water, *Appl. Catal. B Environ.* 94 (2010) 318–326.
- [13] O.M. Daniel, A. Delariva, E.L. Kunkes, A.K. Datye, J.A. Dumesic, R.J. Davis, X-ray absorption spectroscopy of bimetallic Pt-Re catalysts for hydrogenolysis of glycerol to propanediols, *ChemCatChem* 2 (2010) 1107–1114.
- [14] M. Chia, Y.J. Pagan-Torres, D. Hibbitts, Q. Tan, H.N. Pham, A.K. Datye, M. Neurock, R.J. Davis, J.A. Dumesic, Selective hydrogenolysis of polyols and cyclic ethers over bifunctional surface sites on rhodium–rhenium catalysts, *J. Am. Chem. Soc.* 133 (2011) 12675–12689.
- [15] Y. Nakagawa, Y. Shinmi, S. Koso, K. Tomishige, Direct hydrogenolysis of glycerol into 1,3-propanediol over rhenium-modified iridium catalyst, *J. Catal.* 272 (2010) 191–194.
- [16] Y. Amada, Y. Shinmi, S. Koso, T. Kubota, Y. Nakagawa, K. Tomishige, Reaction mechanism of the glycerol hydrogenolysis to 1,3-propanediol over Ir-ReO_x/SiO₂ catalyst, *Appl. Catal. B Environ.* 105 (2011) 117–127.
- [17] Y. Nakagawa, X. Ning, Y. Amada, K. Tomishige, Solid acid co-catalyst for the hydrogenolysis of glycerol to 1,3-propanediol over Ir-ReO_x/SiO₂, *Appl. Catal. A Gen.* 433–434 (433) (2012) 128–.
- [18] S. Koso, H. Watanabe, K. Okumura, Y. Nakagawa, K. Tomishige, Comparative study of Rh-MoO₃ and Rh-ReO_x supported on SiO₂ for the hydrogenolysis of ethers and polyols, *Appl. Catal. B Environ.* 111–112 (111) (2012) 27–.
- [19] K. Tomishige, M. Tamura, Y. Nakagawa, Role of Re species and acid cocatalyst on Ir-ReO_x/SiO₂ in the C–O hydrogenolysis of biomass-derived substrates, *Chem. Rec.* 14 (2014) 1041–1054.
- [20] L. Zhang, A.M. Karim, M.H. Engelhard, Z. Wei, D.L. King, Y. Wang, Correlation of Pt-Re surface properties with reaction pathways for the aqueous-phase reforming of glycerol, *J. Catal.* 287 (2012) 37–43.
- [21] R. Arundhati, T. Mizugaki, T. Mitsudome, K. Jitsukawa, K. Kaneda, Highly selective hydrogenolysis of glycerol to 1,3-propanediol over a boehmite-supported platinum/tungsten catalyst, *ChemSusChem* 6 (2013) 1345–1347.
- [22] S. García-Fernández, I. Gandarias, J. Requies, M.B. Güemez, S. Bennici, A. Auroux, P.L. Arias, New approaches to the Pt/WO_x/Al₂O₃ catalytic system

behavior for the selective glycerol hydrogenolysis to 1,3-propanediol, *J. Catal.* 323 (2015) 65–75.

[23] D. Ferri, T. Bürgi, A. Baiker, Pt and Pt/Al₂O₃ Thin films for investigation of catalytic solid-liquid interfaces by ATR-IR spectroscopy: CO adsorption, H₂-induced reconstruction and surface-enhanced absorption, *J. Phys. Chem. B.* 105 (2001) 3187–3195.

[24] P.R. Griffiths, J.A. de Haseth, The handbook of infrared and Raman characteristic frequencies of organic molecules, in: D. Lin-Vien, N.B. Colthup, W.G. Fateley, J.G. Grasselli (Eds.), *Handb. Infrared Raman Charact. Freq. Org. Mol.*, 2nd ed., John Wiley & Sons, New York, 1991.

[25] R. He, R.R. Davda, J.A. Dumesic, In situ ATR-IR spectroscopic and reaction kinetics studies of water-gas shift and methanol reforming on Pt/Al₂O₃ catalysts in vapor and liquid phases, *J. Phys. Chem. B.* 109 (2005) 2810–2820.

[26] S.D. Ebbesen, B.L. Mojett, L. Lefferts, In situ ATR-IR study of CO adsorption and oxidation over Pt/Al₂O₃ in gas and aqueous phase: promotion effects by water and pH, *J. Catal.* 246 (2007) 66–73.

[27] S.D. Ebbesen, B.L. Mojett, L. Lefferts, In situ ATR-IR study of nitrite hydrogenation over Pd/Al₂O₃, *J. Catal.* 256 (2008) 15–23.

[28] I. Ortiz-Hernández, C.T. Williams, In Situ Investigation of solid-liquid catalytic interfaces by attenuated total reflection infrared spectroscopy, *Langmuir* 19 (2003) 2956–2962.

[29] B.L. Mojett, S.D. Ebbesen, L. Lefferts, Light at the interface: the potential of attenuated total reflection infrared spectroscopy for understanding heterogeneous catalysis in water, *Chem. Soc. Rev.* 39 (2010) 4643–4655.

[30] NIST, Standard Reference Database, (n.d.) <http://webbook.nist.gov/chemistry/name-ser.html>.

[31] K. Koichumanova, K.B. Sai Sankar Gupta, L. Lefferts, B.L. Mojett, K. Seshan, An in situ ATR-IR spectroscopy study of aluminas under aqueous phase reforming conditions, *Phys. Chem. Chem. Phys.* 17 (2015) 23795–23804.

[32] D.A. Boga, F. Liu, P.C.A. Brujinincx, B.M. Weckhuysen, Aqueous-phase reforming of crude glycerol: effect of impurities on hydrogen production, *Catal. Sci. Technol.* 6 (2015) 134–143.

[33] D. Ferri, T. Bürgi, A. Baiker, Probing boundary sites on a Pt/Al₂O₃ model catalyst by CO₂ hydrogenation and in situ ATR-IR spectroscopy of catalytic solid-liquid interfaces, *Phys. Chem. Chem. Phys.* 4 (2002) 2667–2672.

[34] I. Ortiz-Hernández, D.J. Owens, M.R. Strunk, C.T. Williams, Multivariate analysis of ATR-IR spectroscopic data: applications to the solid-liquid Catalytic interface, *Langmuir* 22 (2006) 2629–2639.

[35] M.R. Silverstein, F.X. Webster, D.J. Kiemle, *Spectrometric Identification of Organic Compounds*, 7th ed., Wiley, New York, 2005.

[36] A. Cho, H. Kim, A. Iino, A. Takagaki, T.S. Oyama, Kinetic and FTIR studies of 2-methyltetrahydrofuran hydrodeoxygenation on Ni₂P/SiO₂, *J. Catal.* 318 (2014) 151–161.

[37] J.R. Copeland, X. Shi, D.S. Sholl, C. Sievers, Surface interactions of C2 and C3 polyols with γ-Al₂O₃ and the role of coadsorbed water, *Langmuir* 29 (2013) 581–593.

[38] M. Dömök, M. Tóth, J. Raskó, A. Erdohelyi, Adsorption and reactions of ethanol and ethanol-water mixture on alumina-supported Pt catalysts, *Appl. Catal. B Environ.* 69 (2007) 262–272.

[39] M.I. Zaki, M.A. Hasan, L. Pasupulety, In situ FTIR spectroscopic study of 2-propanol adsorptive and catalytic interactions on metal-modified aluminas, *Langmuir* 17 (2001) 4025–4034.

[40] A.V. Deo, I.G. Dalla Lana, Infrared study of the adsorption and mechanism of surface reactions of 1-propanol on γ-alumina and γ-alumina doped with sodium hydroxide and chromium oxide, *J. Phys. Chem.* 73 (1969) 716–723.

[41] V. Sablinskas, G. Steiner, M. Hof, R. Machán, Applications, in: G. Gauglitz, D.S. Moore (Eds.), *Handb. Spectrosc.*, 2nd ed., Wiley-VCH, Weinheim, 2014, pp. 95–174.

[42] Y. Nakagawa, M. Tamura, K. Tomishige, Catalytic materials for the hydrogenolysis of glycerol to 1,3-propanediol, *J. Mater. Chem. A* 2 (2014) 6688–6702.

[43] B. Stuart, Infrared spectroscopy, in: Kirk-Othmer (Ed.), *Kirk-Othmer Encycl. Chem. Technol.*, 5th ed., Wiley, New York, 2000, pp. 1–20.

[44] S.D. Ebbesen, B.L. Mojett, L. Lefferts, CO adsorption and oxidation at the catalyst-water interface: an investigation by attenuated total reflection infrared spectroscopy, *Langmuir* 22 (2006) 1079–1085.

[45] E.S. Vasiliadou, A.A. Lemonidou, Kinetic study of liquid-phase glycerol hydrogenolysis over Cu/SiO₂ catalyst, *Chem. Eng. J.* 231 (2013) 103–112.

[46] W. Van Bronswijk, H.R. Watling, Z. Yu, A study of the adsorption of acyclic polyols on hydrated alumina, *Colloids Surf. A Physicochem. Eng. Asp.* 157 (1999) 85–94.

[47] M.A. Dasari, P.P. Kiatsimkul, W.R. Sutterlin, G.J. Suppes, Low-pressure hydrogenolysis of glycerol to propylene glycol, *Appl. Catal. A Gen.* 281 (2005) 225–231.

[48] T. Miyazawa, Y. Kusunoki, K. Kunimori, K. Tomishige, Glycerol conversion in the aqueous solution under hydrogen over Ru/C+ an ion-exchange resin and its reaction mechanism, *J. Catal.* 240 (2006) 213–221.

[49] J. TenDam, K. Djanashvili, F. Kapteijn, U. Hanefeld, Pt/Al₂O₃ catalyzed 1,3-propanediol formation from glycerol using tungsten additives, *ChemCatChem* 5 (2013) 497–505.

[50] L. Huang, Y. Zhu, H. Zheng, G. Ding, Y. Li, Direct conversion of glycerol into 1,3-propanediol over Cu-H₄SiW₁₂O₄₀/SiO₂ in vapor phase, *Catal. Lett.* 131 (2009) 312–320.

[51] A.O. Menezes, M.T. Rodrigues, A. Zimmaro, L.E.P. Borges, M.A. Fraga, Production of renewable hydrogen from aqueous-phase reforming of glycerol over Pt catalysts supported on different oxides, *Renew. Energy* 36 (2011) 595–599.

[52] D.L. King, L. Zhang, G. Xia, A.M. Karim, D.J. Heldebrant, X. Wang, T. Peterson, Y. Wang, Aqueous phase reforming of glycerol for hydrogen production over Pt-Re supported on carbon, *Appl. Catal. B Environ.* 99 (2010) 206–213.

[53] L.-Z. Qin, M.-J. Song, C.-L. Chen, Aqueous-phase deoxygenation of glycerol to 1,3-propanediol over Pt/WO₃/ZrO₂ catalysts in a fixed-bed reactor, *Green Chem.* 12 (2010) 1466–1472.

[54] X. Wu, L. Zhang, D. Weng, S. Liu, Z. Si, J. Fan, Total oxidation of propane on Pt/WO_x/Al₂O₃ catalysts by formation of metastable Pt^{δ+} species interacted with WO_x clusters, *J. Hazard. Mater.* 225–226 (2012) 146–154.

[55] D.G. Barton, M. Shtein, R.D. Wilson, S.L. Soled, E. Iglesia, Structure and electronic properties of solid acids based on tungsten oxide nanostructures, *J. Phys. Chem. B* 103 (1999) 630–640.

[56] J. Oh, S. Dash, H. Lee, Selective conversion of glycerol to 1,3-propanediol using Pt-sulfated zirconia, *Green Chem.* 13 (2011) 2004–2007.

[57] S. Zhu, Y. Zhu, S. Hao, L. Chen, B. Zhang, Y. Li, Aqueous-phase hydrogenolysis of glycerol to 1,3-propanediol over Pt-H₄SiW₁₂O₄₀/SiO₂, *Catal. Lett.* 142 (2012) 267–274.

[58] T. Mizugaki, T. Yamakawa, R. Arundhathi, T. Mitsudome, K. Jitsukawa, K. Kaneda, Selective hydrogenolysis of glycerol to 1,3-propanediol catalyzed by Pt nanoparticles-Al₂O_x/WO₃, *Catal. Lett.* 41 (2012) 1720–1722.

[59] S. Zhu, X. Gao, Y. Zhu, Y. Li, Promoting effect of WO_x on selective hydrogenolysis of glycerol to 1,3-propanediol over bifunctional Pt–WO_x/Al₂O₃ catalysts, *J. Mol. Catal. A Chem.* 398 (2015) 391–398.

[60] S. Zhu, Y. Qiu, Y. Zhu, S. Hao, H. Zheng, Y. Li, Hydrogenolysis of glycerol to 1,3-propanediol over bifunctional catalysts containing Pt and heteropolyacids, *Catal. Today* 212 (2013) 120–126.

[61] S. Koso, I. Furikado, A. Shima, T. Miyazawa, K. Kunimori, K. Tomishige, Chemoselective hydrogenolysis of tetrahydrofurfuryl alcohol to 1,5-pentanediol, *Chem. Commun.* (2009) 2035–2037.

[62] S. Koso, Y. Nakagawa, K. Tomishige, Mechanism of the hydrogenolysis of ethers over silica-supported rhodium catalyst modified with rhenium oxide, *J. Catal.* 280 (2011) 221–229.

[63] M.R. Nimlos, S.J. Blanksby, X. Qian, M.E. Himmel, D.K. Johnson, Mechanisms of glycerol dehydration, *J. Phys. Chem. A* 110 (2006) 6145–6156.

[64] D.G. Barton, S.L. Soled, G.D. Meitzner, G.A. Fuentes, E. Iglesia, Structural and catalytic characterization of solid acids based on zirconia modified by tungsten oxide, *J. Catal.* 181 (1999) 57–72.

[65] S. Triwahyono, T. Yamada, H. Hattori, Kinetic study of hydrogen adsorption on Pt/WO₃–ZrO₂ and WO₃–ZrO₂, *Appl. Catal. A Gen.* 250 (2003) 65–73.

[66] A. Alhanash, E.F. Kozhevnikova, I.V. Kozhevnikov, Gas-phase dehydration of glycerol to acrolein catalysed by caesium heteropoly salt, *Appl. Catal. A Gen.* 378 (2010) 11–18.

[67] Y. Amada, H. Watanabe, Y. Hirai, Y. Kajikawa, Y. Nakagawa, K. Tomishige, Production of biobutanediols by the hydrogenolysis of erythritol, *ChemSusChem* 5 (2012) 1991–1999.